Electric-Field-Induced Soft-Mode Hardening in $SrTiO_3$ Films

I. A. Akimov, A. A. Sirenko,* A. M. Clark, J.-H. Hao, and X. X. Xi

Department of Physics, the Pennsylvania State University, University Park, Pennsylvania 16802

(Received 13 December 1999)

We have studied electric-field-induced Raman scattering in $SrTiO_3$ thin films using an indium-tin/oxide/$SrTiO_3$/$SrRuO_3$ structure grown by pulsed laser deposition. The soft mode polarized along the field becomes Raman active. Experimental data for electric-field-induced hardening of the soft modes and the tuning of the static dielectric constant are in agreement described by the Lyddane-Sachs-Teller formalism. The markedly different behavior of the soft modes in thin films from that in the bulk is explained by the existence of local polar regions.

PACS numbers: 63.20.–e, 77.84.Dy

Applications of ferroelectric thin films in microelectronics have initiated a broad interest in their fundamental properties [1,2]. Of central importance is the behavior of the soft mode, i.e., the lowest frequency transverse optical phonon, whose zone-center frequency ω_{TO_1} is connected to the static dielectric constant ϵ_0 via the Lyddane-Sachs-Teller (LST) relationship and vanishes at the temperature of the ferroelectric phase transition [3]. By using far-infrared (far-IR) ellipsometry, we have recently demonstrated that the soft mode in $SrTiO_3$ (STO) thin films has a higher frequency in comparison with that found in bulk crystals, which is consistent with reduction of ϵ_0 in thin films [4]. The response of ϵ_0 to the external electric field, or the dielectric nonlinearity, demonstrates the difference between the dielectric properties of the ferroelectric films and bulk crystals and is crucial for various applications of ferroelectric thin films [5]. In STO single crystals, the dielectric nonlinearity vanishes above $T \sim 80$ K [6] but remains nonzero to very high temperature in thin films [7]. It has been shown that the specifics of tunability in the bulk is due to the field-induced hardening of the soft mode [8], which arises from the anharmonic restoring forces on the Ti ion when it is displaced from its equilibrium position [9]. To understand the dielectric nonlinearity in STO thin films, detailed experimental studies of the soft modes in the presence of electric field are necessary.

Conventional Raman scattering in cubic central-symmetric STO crystals is restricted by the odd parity of the optical phonons of F_{1u} symmetry. Below the structural cubic-to-tetragonal phase transition temperature ($T_a = 105$ K), the soft-mode phonon splits into two components of A_{2u} and E_u symmetry which remain Raman inactive. First order Raman scattering in STO has been observed only when the central symmetry of the crystal is broken by the presence of impurities [10] or applied external electric field [8]. The soft modes have also been seen in the case of uniaxial stress-induced [11] and hydrostatic pressure-induced [12] ferroelectricity and using far-IR spectroscopy [13], neutron scattering [14], and hyper-Raman scattering [15]. In our previous studies of STO thin films grown on $LaAlO_3$ substrates we observed first order Raman scattering by hard-mode TO_2 and TO_4 phonons, while the soft TO_1 mode has not been detected [16,17]. In this paper, we describe Raman scattering experiments in STO thin films grown on STO substrates with a $SrRuO_3$ (SRO) buffer layer in which application of an electric field allowed detailed investigation of the soft modes. We will focus on dependencies of the soft-mode frequencies on electric field and temperature in connection with the electric-field-induced tuning of the static dielectric constant. The soft-mode hardening in the films is discussed in terms of local polarization due to oxygen vacancies, which we believe causes different dielectric properties of thin films from those in bulk crystals.

The measured sample consisted of a 0.2-μm-thick transparent indium-doped tin oxide (ITO) top electrode deposited on a (1-μm-thick STO)/(0.35-μm-thick SRO) bilayer. The entire ITO/STO/SRO trilayer structure was grown using pulsed laser deposition on a single crystal STO substrate [see inset of Fig. 1(a)]. The STO/SRO bilayer was deposited epitaxially at 750 °C in 100 mTorr of oxygen (see Refs. [7,18] for details), while ITO was grown at 200 °C in 16 mTorr oxygen which results in high conductivity of this layer [19]. The ITO top electrode allows both the application of electric field normal to the film plane and the low-frequency measurements of the dielectric constant in the capacitor geometry. The Raman response of the top ITO layer is very weak compared to that of STO films, and the Raman spectra measured from the coated and uncoated parts of the same STO film are essentially identical. The conductive SRO film screens the optical signal from the substrate, and also serves as the bottom electrode. During the optical measurement, a dc voltage was applied to the sample providing a nominal electric field $\mathcal{E}$ up to 25×10^4 V/cm, approximately the breakdown field for the STO film at room temperature. X-ray diffraction measurements demonstrated that STO films have a pseudocubic structure at high temperatures with a transition to a tetragonal structure at about 120 K [20].

Raman scattering measurements were taken in the conventional backscattering and in close-to-90°

0031-9007/00/()/1(4)$15.00

ACC. CODE **LM7391** AUTHOR **akimov** AIP ID **001020PRL**

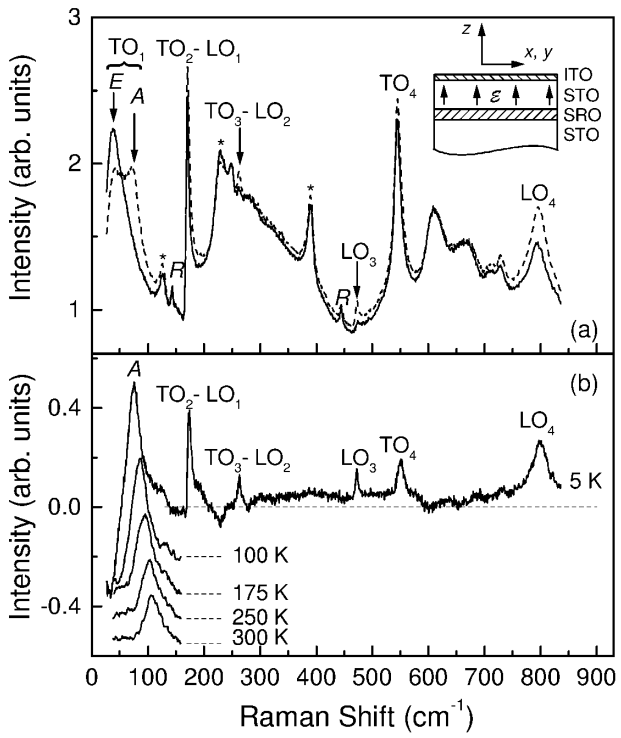

FIG. 1. (a) Solid and dotted lines show the Raman spectra of 1 μm STO film at $T = 5$ K without electric field and in the presence of an external electric field of 22×10^4 V/cm directed normal to the film plane, respectively. The soft-mode components are labeled A and E. Structural modes are denoted by R. Optical phonons from the SRO buffer layer are marked with stars. The inset shows the schematics of the investigated trilayer ITO/STO/SRO structure grown on an STO substrate. (b) Electric-field-induced modification of the Raman intensity obtain by subtracting spectrum at $\mathcal{E} = 22 \times 10^4$ V/cm from that at $\mathcal{E} = 0$ for different temperatures shown next to the spectra. Spectra are shifted vertically for clarity.

configurations. An oblique direction for incident and scattered light was utilized to probe phonons propagating at different angles with respect to the field. The 514.5 nm line of an Ar^+-ion laser was used for excitation. The sample was attached to the cold finger inside an optical He-flow cryostat with a temperature range between 5 and 300 K. Raman spectra were recorded with a SPEX Triplemate spectrometer equipped with a charge-coupled device detector cooled with liquid nitrogen. The resolution was about 1 cm^{-1}. The low-frequency dielectric constant of STO film was measured at 1 kHz using an *LCR* meter.

The Raman spectra obtained with and without electric field at $T = 5$ K are shown in Fig. 1(a). At $\mathcal{E} = 0$, a strong maximum labeled E can be seen at 40 cm^{-1} along with the hard-mode optical phonons. External electric field results in two major effects: the E maximum decreases in intensity and a new peak labeled A arises at about 63 cm^{-1}. The change of the Raman intensity induced by the electric field is presented in Fig. 1(b). The frequency and line shape of the A maximum is similar to that of the IR-active TO_1 phonon we have observed recently by far-IR ellipsometry at zero field in the same sample [4]. The intensity of the A peak is the strongest at oblique incidence in p polarization, when the electric field of exciting and scattered light has a normal component (along the z axis) relative to the surface of the film (x-y plane). This maximum has much weaker intensity in the case of s polarization and is absent in the exact backscattering configuration, when there is no component of the electric field of the exciting or scattered light along $\mathcal{E}$ (z direction). The selection rules for the A and E maxima change with an increase of electric field. In the strong field limit the nonzero components of the Raman tensor are $\alpha_{xz,yz}$ for the E and α_{zz} for the A peaks, the same as those for the E and A_1 phonons in bulk STO with applied electric field in z direction [8]. Thus, the E and A maxima are identified as components of the soft TO_1 mode polarized perpendicular and parallel to the applied field, respectively. At low temperatures, the E and A modes originate from the E_u and A_{2u} phonon states in the bulk, respectively, and the splitting between them in the limit of the low electric field is induced by the tetragonal distortion.

The temperature dependence of the soft-mode frequency for various external electric fields is shown in Fig. 2(a). To extrapolate the frequency of the A mode to zero field [see open symbols in Fig. 2(a)], we used the formula of Fleury and Worlok [8] based on Devonshire's expansion of Gibb's free-energy density [21] and LST relation:

$$\omega^2_{\mathrm{TO}_1}(T,P) = \omega^2_{\mathrm{TO}_1}(T,0) + \Lambda\{3\xi P^2 + 5\eta P^4\}. \quad (1)$$

Here Λ, ξ, and η are parameters in Devonshire's expansion of susceptibility and P is the polarization which is either spontaneous, P_s, or induced by external field, $P_{\mathcal{E}}$. The soft-mode frequency decreases as the temperature is lowered, but instead of saturating at 13 and 20 cm^{-1} for the E_u and A_{2u} phonon states, respectively, as in the bulk crystals [15], in the film it saturates at 40 and 63 cm^{-1} for the E and A modes, respectively [see Fig. 2(a)]. Both E and A phonons shift to higher frequencies with the increase of electric field, i.e., these modes become harder, although the variation of the A component which is polarized along the electric field is much stronger. At low temperature, the increase in A mode frequency is about 30% for an electric field of 25×10^4 V/cm, and the electric-field-induced soft-mode hardening is observed in the entire temperature range of the measurement. This is different from bulk crystals where the tuning of the soft mode disappears above $T \sim 80$ K [8].

At $T = 5$ K the splitting between the A and E soft-mode components is 23 cm^{-1}, about twice as large as that in bulk STO crystals [15]. As expected, this splitting vanishes at the structural transition temperature of $T_a = 120$ K, which has been determined in the Raman scattering experiments [Fig. 2(b)] from dependence of the average intensity of the structural R modes at 144 and 444 cm^{-1}, labeled R in Fig. 1(a). In the films these phonons disappear at about

ACC. CODE **LM7391** AUTHOR **akimov** AIP ID **001020PRL**

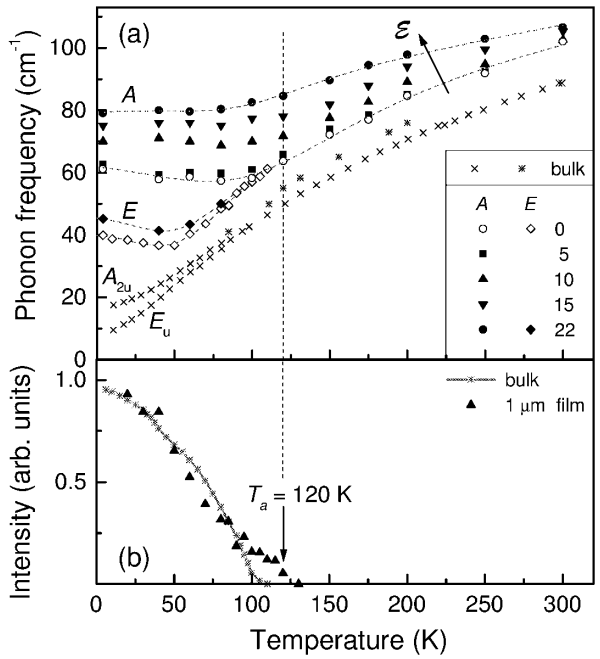

FIG. 2. (a) Frequency of the TO_1 phonon as a function of temperature for different values of external electric field. Zero-field values of the A mode are obtained by extrapolation (see the text for details) and shown with open symbols. The dotted lines guide the eye. Electric-field values are given in 10^4 V/cm. The vertical dashed line indicates the structural cubic-to-tetragonal phase transition in the film at 120 K. Temperature dependence of the soft modes in bulk STO from Refs. [8] (stars) and [15] (crosses) is shown for comparison. (b) Normalized average intensity of the structural R modes at 144 and 444 cm^{-1} as a function of temperature. The stars show the same dependence measured in bulk STO crystal, where the transition temperature is lower: $T_a = 105$ K.

120 ± 5 K, while in the bulk their intensity vanishes at 105 K, as shown in Fig. 2(b). This observation is in quantitative agreement with the x-ray diffraction measurements, demonstrating that the structural transition temperature in STO films is higher than that in the bulk [20]. Above the transition temperature, we did not observe the electric-field-induced splitting of the soft mode due to an increase in the phonon linewidth accompanied by the reduction of the total Raman intensity [17].

Several reasons can be adduced to explain the hardening of the soft mode in thin films. Strain in the film due to the lattice mismatch with the substrate [22] and depolarization field due to discontinuity at the interfaces [23] can, in principle, be responsible for this effect. However, the lattice mismatch in our sample is virtually zero and the induced stress is much smaller than that necessary to change significantly the soft-mode frequency in bulk STO [11]. The interface effects are presumably weak and should not affect the entire volume of the 1-μm-thick film probed in the Raman scattering experiments. Therefore, we propose another explanation based on intrinsic properties of the film material modified for the presence of structural defects. It is well known that the most common defects in titanates are oxygen vacancies [24] resulting from impurities and cation nonstoichiometry [25]. It has been shown that the oxygen vacancies give rise to the appearance of local polar regions, and a quasistatic polarization P_s can be associated with them [26]. This polarization causes an increase in the soft-mode frequency in the film as evident from Eq. (1). For the case of $\mathcal{E} = 0$, when in a perfect paraelectric bulk STO crystal $P_s = 0$, the difference between the soft-mode frequencies in the film, $\omega_{\mathrm{TO}_1}(T, P_s)$, and in the bulk, $\Omega_{\mathrm{TO}_1}(T)$, can be written as

$$\omega^2_{\mathrm{TO}_1}(T, P_s) - \Omega^2_{\mathrm{TO}_1}(T) \propto \langle P_s^2(T) \rangle , \qquad (2)$$

where $\langle P_s^2(T) \rangle$ is the mean square of polarization averaged over the length scale comparable to the wavelength of the soft-mode phonon. This formula is obtained in the spirit of the theoretical approach of Vendik *et al.* [23] and Vogt [27], which has also explained the hardening of the soft modes in bulk $KTaO_3$ induced by doping with Li [27]. The effect of external electric field on the soft-mode frequency in the films can be taken into account in the same manner via the expansion of the additional field-induced polarization $P_{\mathcal{E}}$ in odd powers of $\mathcal{E}$. In this scenario, our results suggest that at low temperatures the influence of polarization P_s is strong because the soft modes in the film are much harder than that in the bulk. The difference between ω_{TO_1} and Ω_{TO_1} is about 30–40 cm^{-1}, which corresponds to an increase of ω_{TO_1} by a factor of 3. The influence of external electric field is relatively weak compared to the effect produced by the local polar regions. In contrast, at high temperatures the soft-mode frequencies in the film and the bulk are close at $\mathcal{E} = 0$, and the difference between them is about 10 cm^{-1}. In this case the maximal electric-field-induced additional polarization in the film $P_{\mathcal{E}}$ is comparable to P_s. This model allows us to connect the hardening of the soft modes in STO films with the concentration of the local polar regions and the electric-field-induced modification of the spatial correlation between electric dipole momenta associated with oxygen vacancies. Note that the existence of the local polar regions in our films is additionally confirmed by the observation of the first order Raman scattering in the case of $\mathcal{E} = 0$ [17]. Indeed, the local polarization breaks the central symmetry of STO films, which explains the Raman activity of the optical phonons.

We have also measured the electric-field-induced changes in the spectra of the hard modes shown in Fig. 1(a). The frequencies of the TO_2 (170 cm^{-1}), TO_4 (545 cm^{-1}), and LO_4 (795 cm^{-1}) phonons [16,17], are almost independent of the field within our experimental accuracy. Only a small hardening of TO_2 phonon by the electric field (of about 1 cm^{-1}) has been detected and it can be attributed to the coupling between the TO_2 and the soft TO_1 mode. In the exact backscattering configuration (the propagation of the scattered phonons is along $\mathcal{E}$), we observed field-induced scattering by longitudinal phonons only. It provided clear determination of the LO_1 phonon frequency which coincides with the TO_2 phonon

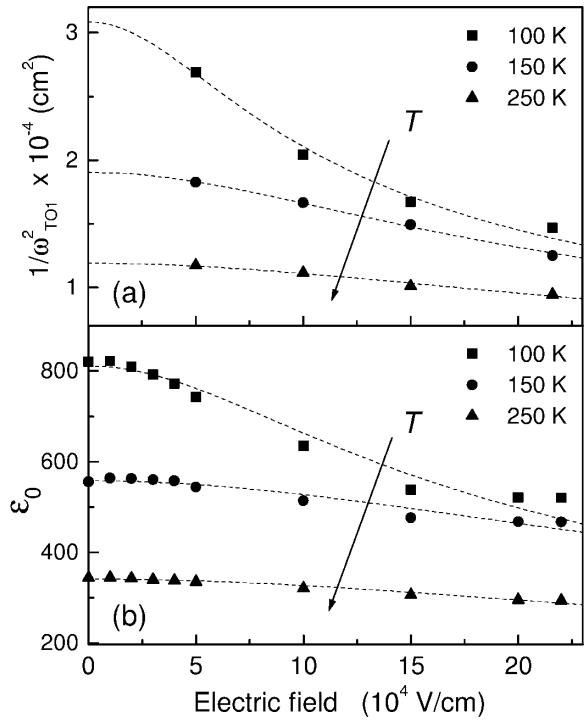

FIG. 3. The inverse square of the soft-mode frequency (a) and static dielectric constant (b) versus electric field measured at different temperatures. (a) and (b) correspond to the right- and left-hand sides of Eq. (3), respectively. The solid lines are results of the fit described in the text.

within our accuracy demonstrating the same behavior as in the bulk. The weak Raman features corresponding to the silent mode at 262 cm^{-1} (degenerate TO_3 and LO_2 phonons) and LO_3 phonon at 472 cm^{-1} become very pronounced upon application of electric field.

The measured electric-field dependence of the soft-mode frequency is consistent with the dielectric nonlinearity in STO thin films. Since the frequencies of phonons other than the soft mode do not change much with electric field and temperature, the LST relation leads to the following simplified expression:

$$\epsilon_0(T,\mathcal{E}) \propto 1/\omega^2_{\mathrm{TO}_1}(T,\mathcal{E}). \qquad (3)$$

Here we neglected the splitting of the soft mode in the tetragonal phase. Figures 3(a) and 3(b) show experimental dependencies of $\omega^{-2}_{\mathrm{TO}_1}(\mathcal{E})$ and $\epsilon_0(\mathcal{E})$ for different temperatures close and above T_a. The remarkable similarity between these data allows us to argue that the mechanisms of electric-field tunability of ϵ_0 in STO films is, as in the bulk, due to electric-field-induced hardening of the soft mode. In principle, this statement is correct for the case of the low temperatures as well. However, our experimental data show that, to describe the contribution of the split soft modes into static dielectric function, a theoretical analysis more elaborate than the simplified LST relation is required. We found that the averaged frequency of the *A* and *E* modes should be used in Eq. (3), taking into account their exact symmetry and alignment of the local polar regions, which both change with electric field.

In conclusion, we have demonstrated that the soft-mode frequency in the thin films is higher than in bulk crystals, and it increases with electric field in the temperature range between 5 and 300 K. The hardening of the soft modes is consistent with the different dielectric constant and dielectric nonlinearity in the films as compared to that in bulk crystals. The soft-mode behavior in the films can be explained qualitatively by the existence of local polar regions induced by oxygen vacancies.

The authors would like to thank C. Bernhard, W. Kleemann, and H. Vogt for helpful discussions. This work was partially supported by DOE under Grant No. DFFG02-84ER45095 and by NSF under Grant No. 9702632.

*Corresponding author.
Email address: sirenko@phys.psu.edu

[1] J. F. Scott and C. A. Paz de Araujo, Science **246**, 1400 (1989).
[2] O. Auciello *et. al.*, Phys. Today **51**, 22 (1998).
[3] W. Cochran, Adv. Phys. **9**, 387 (1960).
[4] A. A. Sirenko *et. al.* (to be published).
[5] X. X. Xi *et. al.* (unpublished).
[6] J. Hemberger *et. al.*, Phys. Rev. B **52**, 13 159 (1995).
[7] H.-Ch. Li *et. al.*, Appl. Phys. Lett. **73**, 190 (1998).
[8] J. M. Worlock and P. A. Fleury, Phys. Rev. Lett. **19**, 1176 (1967); P. A. Fleury and J. M. Worlock, Phys. Rev. **174**, 613 (1968).
[9] G. Rupprecht *et. al.*, Phys. Rev. **123**, 97 (1961).
[10] W. Kleemann *et. al.*, Ferroelectrics **203**, 57 (1997).
[11] H. Uwe and T. Sakodo, Phys. Rev. B **13**, 271 (1976).
[12] T. Ishidate and T. Isonuma, Ferroelectrics **137**, 45 (1992).
[13] J. L. Servoin *et. al.*, Phys. Rev. B **22**, 5501 (1980).
[14] J. D. Axe *et. al.*, Phys. Rev. B **1**, 1227 (1970).
[15] H. Vogt, Phys. Rev. B **51**, 8046 (1995).
[16] V. I. Merkulov *et. al.*, Appl. Phys. Lett. **72**, 3291 (1998).
[17] A. A. Sirenko *et. al.*, Phys. Rev. Lett. **82**, 4500 (1999).
[18] H.-Ch. Li *et. al.*, Appl. Phys. Lett. **73**, 464 (1998).
[19] J. P. Zheng and H. S. Kwok, Appl. Phys. Lett. **63**, 1 (1993).
[20] Wells *et al.* (unpublished).
[21] A. F. Devonshire, Philos. Mag. **40**, 1040 (1949).
[22] I. Fedorov *et. al.*, Ferroelectrics **208–209**, 413 (1998).
[23] O. G. Vendik *et al.*, J. Appl. Phys. **84**, 993 (1998).
[24] R. Waser and D. M. Smyth, in *Ferroelectric Thin Films: Synthesis and Basic Properties*, edited by C. P. de Araujo *et. al.* (Gordon and Breach, Amsterdam, 1996), p. 47.
[25] S. K. Streiffer *et. al.*, J. Appl. Phys. **86**, 4564 (1999).
[26] C. Fischer *et. al.*, Radiat. Eff. Defects Solids **136**, 85 (1995).
[27] H. Vogt, J. Phys. Condens. Matter **7**, 5913 (1995); H. Vogt, Ferroelectrics **202**, 157 (1997).